Senescent Leaves of *Artemisia annua* are One of the Most Active Organs for Overexpression of Artemisinin Biosynthesis Responsible Genes upon Burst of Singlet Oxygen

Authors Rui-Yi Yang[1]*, Xiao-Mei Zeng[1]*, Yuan-Yuan Lu[2], Wen-Jie Lu[1], Li-Ling Feng[3], Xue-Qin Yang[3], Qing-Ping Zeng[1]

Affiliations
[1] Laboratory of Biotechnology, Tropical Medicine Institute, Guangzhou University of Chinese Medicine, Guangzhou, P. R. China
[2] Laboratory of Pharmacology, Tropical Medicine Institute, Guangzhou University of Chinese Medicine, Guangzhou, P. R. China
[3] Artemisinin Research Center, Guangzhou University of Chinese Medicine, Guangzhou, P. R. China

Key words
- *Artemisia annua*
- Asteraceae
- artemisinin
- oxidative stress
- singlet oxygen
- induction
- expression profile

Abstract

To dissect and penetrate complexicity regarding the tissue-specific and environment-induced expression modes of cytosolic and plastidial terpene biosynthetic genes in *A. annua*, corresponding mRNAs relevant to terpene biosynthesis were quantitatively compared among distinctive organs and during different growth stages. Although all examined mRNAs gradually elevate from June to August in tested organs, a putative artemisinin biosynthesis responsible *DBR2* mRNA represents the most abundant transcript anyplace and anytime. Apart from others, senescent leaves endow global activation of artemisinin biosynthetic genes and ultimately lead to enhanced artemisinin production. Direct measurement of $^1O_2$ burst from senescent leaves strongly supports an involvement of $^1O_2$ in conversion from precursor (s) to artemisinin. In the context of environmental stresses, physical and chemical stress signals that include those invoking $^1O_2$ burst were evaluated as if inducing artemisinin biosynthetic genes. The quantitative data have reiterated a common pattern of modulating artemisinin production in *A. annua* by triggering $^1O_2$ burst during senescence and under chilling acclimatization. In conclusion, a missing link concatenating senescence-coupled $^1O_2$ generation to $^1O_2$-induced upregulation of artemisinin biosynthetic genes has been re-established, which would provide a fertile base for future endeavors pursuing further enhancements of artemisinin production.

Abbreviations

ADS:	amorphadiene synthase
CPR:	cytochrome P450 reductase
CYP71AV1:	cytochrome P450 monooxygenase
DBR2:	Δ 11(13) double-bond reductase 2
DHAA:	dihydroartemisinic acid
FDS/FPS:	farnesyl diphosphate synthase
HMGR:	3-hydroxyl-3-methylglutaryl coenzyme A reductase
MS:	Murashige and Skoog
MVA:	mevalonic acid
SS/SQS:	squalene synthase

received February 10, 2009
revised July 30, 2009
accepted October 27, 2009

Bibliography
DOI http://dx.doi.org/10.1055/s-0029-1240620
Published online November 25, 2009
Planta Med 2010; 76: 734–742

ISSN 0032-0943

Correspondence
Prof. Dr. Qing-Ping Zeng
Laboratory of Biotechnology
Tropical Medicine Institute
Guangzhou University of Chinese Medicine
No. 12, Airport Road
510405 Guangzhou
People's Republic of China
Phone: + 86 20 36 58 51 00
Fax: + 86 20 86 35 43 29
qpzeng@gzhtcm.edu.cn

Introduction

Since the antimalarial agent artemisinin was purified from *A. annua* (Asteraceae) early in 1970s [1], explorations pursuing enhanced artemisinin production have been launched [2,3]. A full understanding of enzymes and encoding genes involved in artemisinin biosynthesis is obviously beneficial to reach the goal of more yield and less cost in artemisinin production [4,5]. Artemisinin is synthesized via the cytosolic mevalonic acid (MVA) pathway in cooperation with the plastidial non-MVA pathway [6]. As a first diverting enzyme, amorphadiene synthase (ADS) converts a linearized farnesyl diphosphate to a cyclic sesquiterpene amorpha-4,11-diene [7]. Afterwards, cytochrome P450 monooxygenase (CYP71AV1) oxidizes amorpha-4,11-diene to artemisinic alcohol, artemisinic aldehyde, and artemisinic acid sequentially by three steps of oxidation processes [8]. All those intermediates were detected in *A. annua* as well as engineered microbes expressing *ADS, CYP71AV1* and *CPR* genes [9–11]. Following expression of a novel cDNA encoding Δ 11(13) double-bond reductase 2 (DBR2) cloned from a tailoring gene library of *A. annua*, both dihydroartemisinic acid (DHAA) and artemisinic acid were identified in the engineered yeast strain that expresses *ADS, CYP71AV1, CPR* and *DBR2* genes [12]. However,

* These authors contributed equally to the present work.

no artemisinin has been isolated from any engineered microbes currently available.

DHAA, an abundant intermediate resided in *A. annua*, has been postulated as a direct precursor of artemisinin, towards which an unstable DHAA hydroperoxide forms via a non-enzymatic step [13, 14]. A correlation between decrease of DHAA content and synchronously increase of artemisinin yield has been established in *A. annua* [15], implying DHAA is a direct precursor of artemisinin. Although artemisinic acid and other derivatives such as arteannuin B and artemisitene were considered as candidate precursors that may also convert to artemisinin [16, 17], no direct evidence has been documented so far.

Furthermore, DHAA has been suggested as a scavenger of singlet oxygen ($^1O_2$) like carotenoids, which bear importance in protecting plastids and perhaps cells themselves from reactive oxygen species [18]. As a putative $^1O_2$ quencher, DHAA may directly react with $^1O_2$ to generate a transition state DHAA hydroperoxide, thereby enabling its spontaneous conversion to artemisinin [19]. However, whether $^1O_2$ affects artemisinin biosynthetic genes and how $^1O_2$ modulates these genes are poorly understood. We have recently shown that low temperature upregulates *ADS* and *CYP71AV1* genes by activating the Ca^{2+}-mediated signal transduction pathway and simultaneously enhances artemisinin production [20, 21], suggesting that oxidative stress is involved in artemisinin biogenesis.

Although some clues indicate developmental and environmental impacts on artemisinin accumulation in senescent leaves of *A. annua* on the basis of metabolite analysis [22], a detailed regulatory mode of action in regard to that artemisinin biosynthesis is regulated at the transcriptional and post-transcriptional levels remains unknown. Moreover, it also necessitates elucidation of the mechanism behind senescence-activating artemisinin biosynthetic genes.

We present here spatial and temporal profiles on the transcription and translation of artemisinin biosynthetic genes by measuring levels of mRNAs and enzymes during different developmental stages with a focus on the comparison of those between green leaves and senescent leaves. We also try to draw a conclusion associating senescence-triggering $^1O_2$ burst with the oxidative stress-mediated upregulation of artemisinin biosynthetic genes as well as artemisinin overproduction.

Materials and Methods

Plant materials

A cultivar (Huayang No. 1) of *A. annua* was grown in the medicinal plant garden at the campus of Guangzhou University of Chinese Medicine and vouched for by Professor Hong He from the College of Herbal Medicine in this University. To obtain *in vitro* cultured plantlets, seeds were harvested from garden-grown plants and disinfected first by soaking in 70% ethanol for 30 sec, then immersing in 3% sodium hypochlorite for 30 min, and finally rinsing with double-distilled water (ddH_2O) for 4–5 times. Sterilized seeds were germinated on the phytohormone-free solid Murashige and Skoog (MS) medium (1/2 MS salts supplemented with vitamins, 30 g/L sucrose and 8 g/L agar powder) in a luminescent growth chamber equipped with fluorescent lamps (≥ 3000 lx) at 25 °C under a photoperiod of 16 h light and 8 h dark. Seedlings or nascent leaves on explants were subcultured onto 400 mL of solid medium in 1000-mL flasks (one cutting in each flask) every four weeks. All treatments were conducted using plantlets cultured for 30 d after subculturing.

Stress treatments of plants cultured *in vitro*

In vitro cultured plants were subjected to different types of stress treatments by dividing them into a physical stress group and a chemical stress group. Three 30-day-old plants were employed for each treatment and three samples were collected from an individual plant. Whole plants were included in treatments, but only leaves were collected for analysis. Unless indicated elsewhere, the flask with a treated plant was generally placed in a 25 °C luminescent chamber with fluorescent lamps (≥ 3000 lx).

The physical stress group included six treatments: (a) low temperature: a flask with a plant to be treated was kept in a 4 °C luminescent chamber with fluorescent lamps (≥ 3000 lx) for 24 h; (b) heat shock: a flask with a plant to be treated was kept first in a 40 °C water bath for 30 min, then in a 25 °C luminescent chamber (≥ 3000 lx) for 2 h, and finally in a 50 °C water bath for 1 h; (c) ultraviolet light: a plant to be treated was kept under the ultraviolet lamp (254 nm, 20 W), 20 cm distant from the light source, for 1 h; (d) waterlogging: roots of a plant to be treated were immersed in ddH_2O at 2 cm in depth for 24 h; (e) dehydration: roots of a plant to be treated were first immersed in ddH_2O at 2 cm in depth for 6 h, and then transferred onto a filter paper for 6 h drying; (f) rehydration: after dehydration, roots of a treated plant were again immersed in ddH_2O at 2 cm in depth for 12 h.

The chemical stress group included three treatments: (a) glucose: a plant to be treated was cultured in the liquid MS medium containing 3% glucose for 7 d; (b) NaCl: a plant to be treated was cultured in the liquid MS medium containing 250 mM NaCl for 48 h; (c) yeast extracts: a plant to be treated was cultured in the liquid MS medium containing 50 mg/L yeast extracts for 7 d.

Quantification of mRNAs and enzymes

100 mg of plant organs were collected from *A. annua* and immediately frozen in liquid nitrogen. For development-specific profiling, leaves were collected from middle parts of plants on 15 June, 15 July, 15 August and 15 September, respectively. For tissue-specific profiling, tissues including roots, stems, leaves, flowers and flower buds were separately pooled on 15 September.

Total RNAs were isolated by a commercially available Plant RNA Kit (Promega). Reverse transcription and real-time fluorescent quantitative polymerase chain reaction were performed with the purchased RevertAid H Minus First Strand cDNA Synthesis Kit (Fermentas) and SYBR Green Real Time PCR Master Mix (TOYOBO) as described [23]. For quantitative analysis, 18S rRNA was chosen as an inner reference. The standard curves of 18S rDNA and target cDNAs were plotted with corresponding recombinant plasmids being constructed in this laboratory. The primers designed for amplifying target genes of *A. annua* were listed in **Table 1**. The relative mRNA level was defined as specific mRNA copy numbers/18S rRNA copy numbers.

Total proteins were isolated from distinctive organs of *A. annua* by the purchased Plant Protein Extraction Kit (Pierce) according to the manufacturer's instructions. Preparation of recombinant antigens in *Escherichia coli*, induction for polyclonal antibodies against recombinant antigens in rabbits, enzyme-linked immunosorbent assay-based immunoquantification were performed as previously described [24]. The relative enzyme concentration (μg/mL) was represented by the amount of a specific enzyme/the volume of a total protein solution.

Table 1 The primers designed for quantitative amplification of selective *A. annua* genes.

Tested genes		Primers		Amplicon length (bp)
Name	**GenBank accession number**	**Name**	**Sequence**	
HMGR	U14625	HMGR-3	5′-GCACAGTTGGAGGAGGGACA-3′	100
		HMGR-4	5′-TGAGCGTTTGAGCCTGGTG-3′	
FPS	U36376	FPS-3	5′-TTCTTTCATCTGCCCTTGGTT-3′	100
		FPS-4	5′-GGTTGCCCTCTGCGTGTATG-3′	
ADS	DQ241826	ADS-7	5′-AGTTTGTTAGAAACCTGATGGTTGAA-3′	105
		ADS-8	5′-GGTTAGCACCGCCAGTAATGA-3′	
CYP71AV1	DQ872632	CYP-3	5′-TGGTTCTGCCAAGAGAGTGC-3′	102
		CYP-4	5′-GGTCCCTATTTATCGCAAAGACG-3′	
CPR	DQ984181	CPR-3	5′-GATAACGAAGACGGGACACCA-3′	102
		CPR-4	5′-GCTCAAAACATCGGCATAGGA-3′	
DBR2	EU848577	DBR-5	5′-CTCAAGGGGATGCTGATTTG-3′	150
		DBR-6	5′-GGTAATCCGTGTACCCAACG-3′	
DXS	AF182286	DXS-3	5′-GACTGGAAGAAGAGACCAAATGC-3′	101
		DXS-4	5′-GACCCGTGCCAAAACAATCA-3′	
DXR	AF182287	DXR-3	5′-GGCATTCAAACCACAGTTAGTCTC-3′	117
		DXR-4	5′-ACAACACCTTCATCACCAGGAA-3′	
SS	AY445506	SQS-3	5′-CGGACTAAAACAATGGCTGATG-3′	104
		SQS-4	5′-GTGATGGTCGTTTGGGCATT-3′	
18S rRNA	Not accessed	18S-3	5′-GCAACAAACCCCGACTTCTG-3′	102
		18S-4	5′-TGCGATCCGTCGAGTTATCA-3′	

Determination of artemisinin

Leaves were toasted in a 50 °C oven for 24 h and ground into fine powder. Artemisinin was determined by high-performance liquid chromatography as described [23]. To prepare the positive control, 10 mg of artemisinin (Sigma; 98 %) were dissolved in methanol, and the concentration of artemisinin was calibrated to 0.4 mg/µL. For plotting a standard curve, aliquots of 2, 4, 8, 12, 16, and 20 µL of the known concentration of artemisinin were individually injected into the sampling outlet of the instrument (Dionex-100). Artemisinin content (mg/g) was defined as the amount of artemisinin/dry weight of plant material.

Spectrophotometric assay of $^1O_2$

$^1O_2$ burst from leaves was monitored by a spectrophotometric method [25] with modifications, in which *N,N*-dimethyl-*p*-nitrosoaniline (Sigma) was used as a selective acceptor of $^1O_2$, and the bleaching of *N,N*-dimethyl-*p*-nitrosoaniline was spectrophotometrically measured at the wavelength of 440 nm. For assay, 450 mg of leaves were collected, sheared into strips with 1 mm width, and put into 5-mL assay mixture containing 45 mM phosphate buffered saline (pH 7.1), 10 mM histidine (Sigma) and 50 µM *N,N*-dimethyl-*p*-nitrosoaniline. Following incubation at 30 °C for 30 min under the extensive light (≥ 3000 lx), 1.5 mL of the reaction solution were applied for determination of the absorbance at 440 nm (A_{440}) with an interval of 30 min during a test session of 2.5–3 h.

Data analysis

All analytical data were expressed as the means ± standard deviations (SD) from three biological replicates with three samples each, unless specifically indicated elsewhere. Only positive SD values were illustrated as error bars in figures. Statistical analysis of *F* test (analysis of variance, ANOVA) was performed with the SPSS 11.5 for windows software package (Statistica).

Results

To elucidate the tissue-specific expression patterns of terpene biosynthetic genes in *A. annua*, corresponding transcripts in major organs of blooming plants were quantitatively analyzed. Of these, seven transcripts coding for MVA pathway enzymes and two transcripts for non-MVA pathway enzymes were compared among five organs. Quantitative results of relative mRNA levels are illustrated in **Fig. 1 A** to **C**. Among organs collected in September, the most abundant transcript is *DBR2* mRNA (5×10^{-5}) (**Fig. 1 A**), while the least abundant transcripts are *FDS* mRNA (0.02×10^{-5}) and *HMGR* mRNA (0.01×10^{-5}) (**Fig. 1 C**). *DBR2* mRNA is, in a maximal level, 90-, 13- and 5-fold higher than *CYP71AV1, ADS* and *CPR* mRNAs (**Fig. 1 A** and **B**). The drastic upregulation of *DBR2* gene in all tested organs suggests that reduction of the C11–C13 double-bond catalyzed by DBR2 is one of the most active reaction steps under investigation. In contrast, due to the occurrence of scarce mRNAs, *HMGR* and *FDS* genes may represent upstream controlling steps on the MVA pathway, while *CYP71AV1* and *ADS* genes are likely downstream rate-limiting checkpoints towards artemisinin biosynthesis.

In a follow-up detection of seven MVA pathway mRNAs and two non-MVA pathway mRNAs from June to September in 2008, dynamic changes of transcripts in leaves were recorded on the monthly basis. As noted from **Fig. 2**, *DBR2* mRNA constantly increased until the last month of analysis. However, other transcripts gradually increased from June, reached the maximum in August, and sharply declined in September. As being distinguishable from others in their maximal levels, *DBR2* mRNA (2.9×10^{-5}), *CPR* mRNA (1.6×10^{-5}) and *ADS* mRNA (0.9×10^{-5}) are more plentiful (**Fig. 2 A**); *DXS* mRNA (0.58×10^{-5}), *SS* mRNA (0.20×10^{-5}) and *CYP71AV1* mRNA (0.18×10^{-5}) remain moderate levels (**Fig. 2 B**); *DXR* mRNA (0.19×10^{-5}), *HMGR* mRNA (0.12×10^{-5}) and *FDS* mRNA (0.06×10^{-5}) represent rare transcripts (**Fig. 2 C**). These results have manifested that activation of cytosolic and plastidial pathway genes are development-dependent,

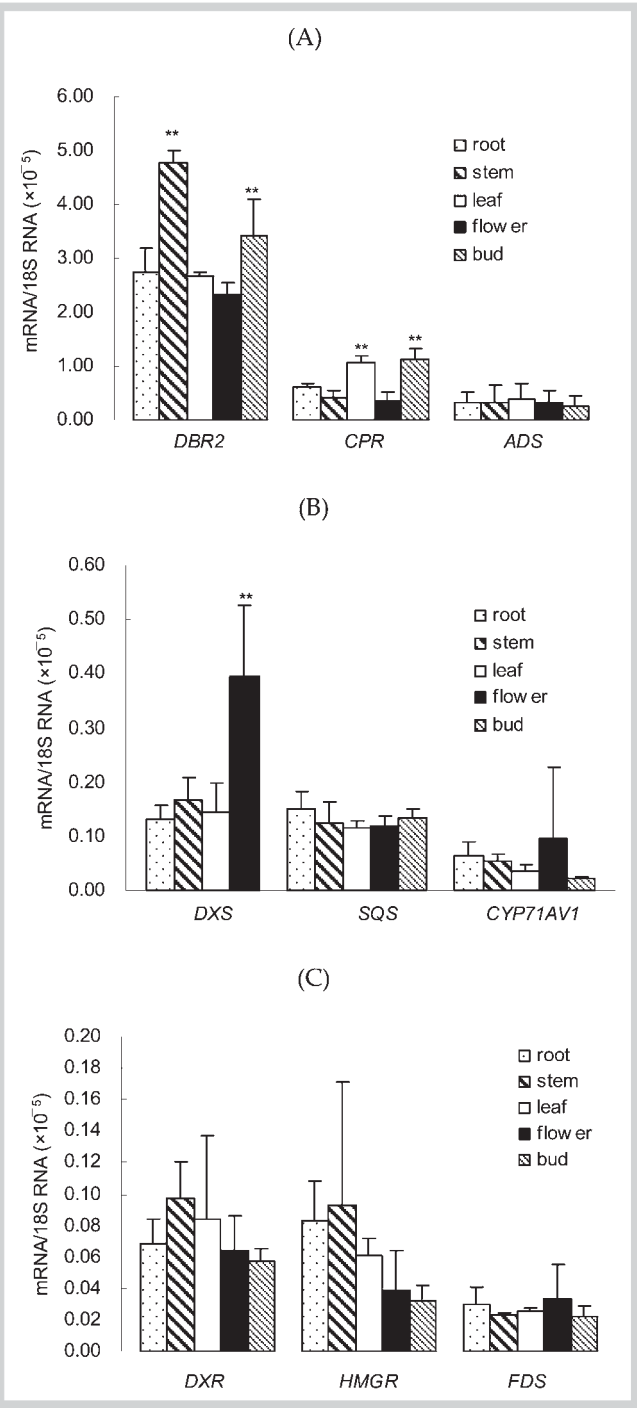

Fig. 1 Quantification of artemisinin biosynthesis responsible mRNAs in distinct organs of wild-grown *A. annua* in September, 2008. **A** The abundant mRNA species; **B** the moderate mRNA species; **C** the rare mRNA species. Copy numbers of each mRNA were estimated according to the regression formula from the standard curve of an individual gene. For 18S rDNA, Y = − 3.281769X + 38.934578, R^2 = 0.993882; For *HMGR*, Y = − 3.344985X + 38.589870, R^2 = 0.996925; For *FPS*, Y = − 3.393294X + 35.677765, R^2 = 0.996712; For *ADS*, Y = − 3.378548X + 39.118325, R^2 = 0.996767; For *CYP71AV1*, Y = − 3.457978X + 37.969635, R^2 = 0.997332; For *CPR*, Y = − 3.483031X + 38.996731, R^2 = 0.999362; For *DBR2*, Y = − 3.847960X + 44.088917, R^2 = 0.998057; For *SQS*, Y = − 3.492085X + 39.390491, R^2 = 0.998876; For *DXS*, Y = − 3.587049X + 40.033127, R^2 = 0.990662; For *DXR*, Y = − 3.572425X + 39.707245, R^2 = 0.994868. Double asterisks (**) represent a very significant statistical difference ($p < 0.01$).

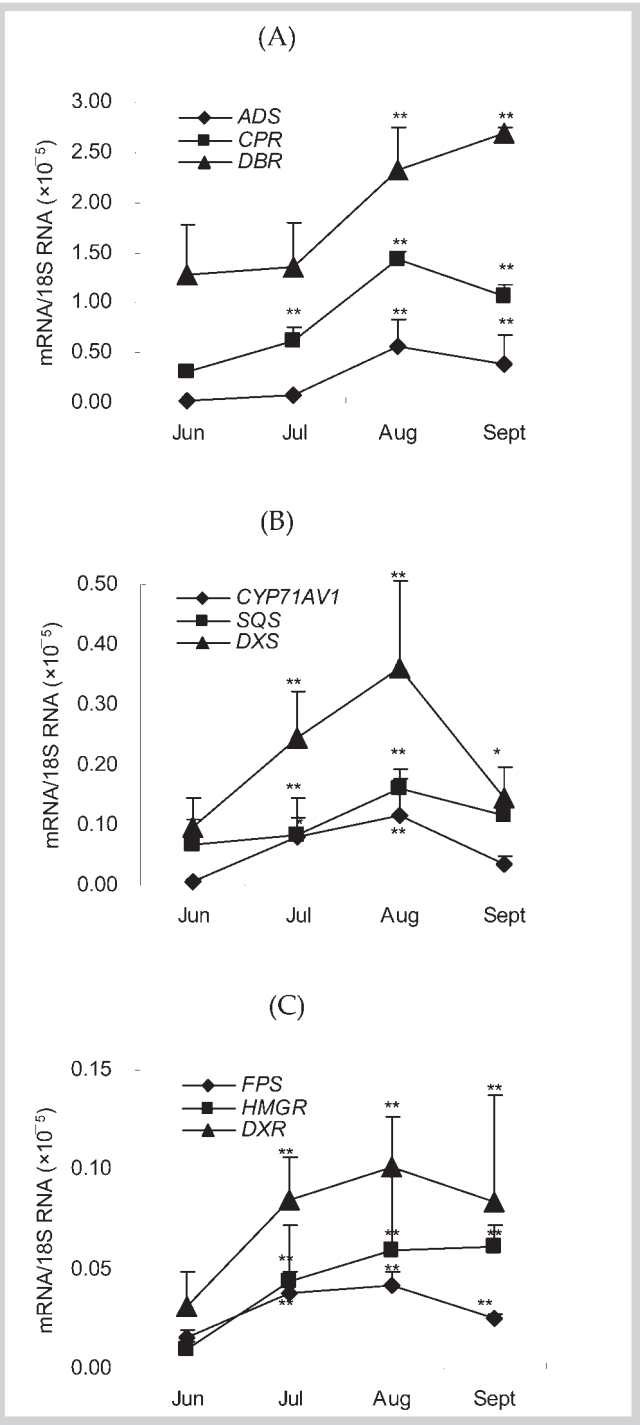

Fig. 2 Quantification of artemisinin biosynthesis responsible mRNAs in leaves of wild-grown *A. annua* from June to September, 2008. **A** The abundant mRNA species; **B** the moderate mRNA species; **C** the rare mRNA species. Copy numbers of each mRNA were estimated according to the regression formula from the standard curve of an individual gene. For 18S rDNA, Y = − 3.150117X + 37.999008, R^2 = 0.994335; For *HMGR*, Y = − 3.476657X + 39.523457, R^2 = 0.997848; For *FPS*, Y = − 3.389733X + 35.215302, R^2 = 0.997412; For *ADS*, Y = − 3.224546X + 38.216091, R^2 = 0.998369; For *CYP71AV1*, Y = − 3.476058X + 38.277225, R_2 = 0.996758; For *CPR*, Y = − 3.476720X + 38.277225, R^2 = 0.998181; For *DBR2*, Y = − 3.847960X + 44.088917, R^2 = 0.998057; For *SQS*, Y = − 3.490311X + 39.407974, R^2 = 0.999183; For *DXS*, Y = − 3.651419X + 40.314491, R^2 = 0.991474; For *DXR*, Y = − 3.528084X + 36.050751, R^2 = 0.993824. The single asterisk (*) represents a significant statistical difference ($p < 0.05$); Double asterisks (**) represent a very significant statistical difference ($p < 0.01$).

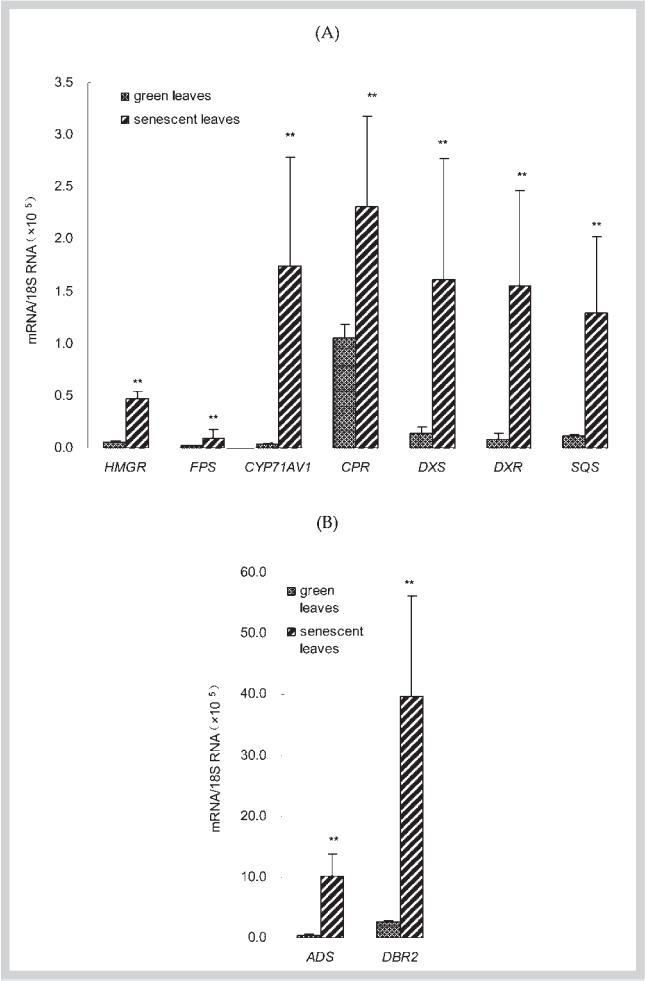

Fig. 3 Quantification of artemisinin biosynthesis responsible mRNAs in green leaves and senescent leaves of wild-grown *A. annua* in September, 2008. **A** The low-level mRNA species; **B** The high-level mRNA species. Copy numbers of each mRNA were estimated according to the regression formula from the standard curve of an individual gene. For 18S rDNA, Y = − 3.281769X + 38.934578, R^2 = 0.993882; For *HMGR*, Y = − 3.344985X + 38.589870, R^2 = 0.996925; For *FPS*, Y = − 3.393294X + 35.677765, R^2 = 0.996712; For *ADS*, Y = − 3.378548X + 39.118320, R^2 = 0.996767; For *CYP71AV1*Y = − 3.457978X + 37.969635, R^2 = 0.997332; For *CPR*, Y = − 3.479555X + 38.889797, R^2 = 0.999238; For *DBR2*, Y = − 3.873987X + 44.862797, R^2 = 0.997820; For *SQS*, Y = − 3.492085X + 39.390491, R^2 = 0.998876; For *DXS*, Y = − 3.587049X + 40.033127, R^2 = 0.990662; For *DXR*, Y = − 3.572425X + 39.707245, R^2 = 0.994868. Double asterisks (**) represent a very significant statistical difference ($p < 0.01$).

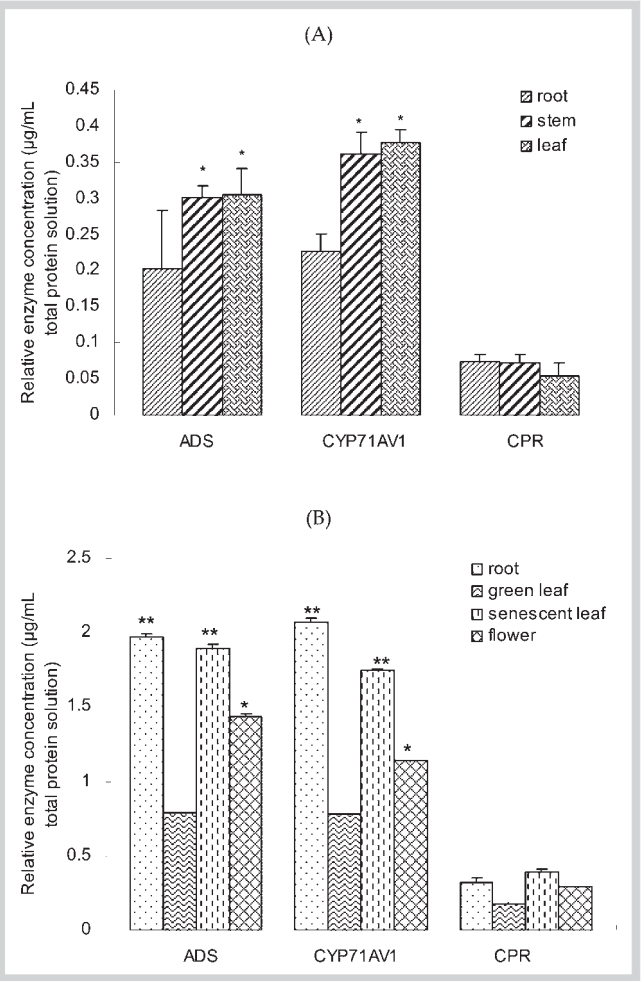

Fig. 4 Quantification of artemisinin biosynthesis responsible enzymes in distinctive organs of wild-grown *A. annua* in September, 2008. **A** On the pre-blooming stage; **B** On the post-blooming stage. Amounts of each enzyme were estimated according to the regression formula from the standard curve of an individual enzyme. For ADS, Y = 0.2002X + 0.0938, R^2 = 0.9846; For CYP71AV1, Y = 0.198X + 0.0836, R^2 = 0.9962; For CPR, Y = 0.7422X + 0.068, R^2 = 0.9924. The single asterisk (*) represents a significant statistical difference ($p < 0.05$); Double asterisks (**) represent a very significant statistical difference ($p < 0.01$).

regardless of the fact that the maximal levels of all transcripts are totally different.

To investigate the development-dependent regulatory patterns of cytosolic and plastidial pathway genes, seven MVA pathway mRNAs and two non-MVA pathway mRNAs were compared between young (green) leaves and senescent (brown and dry) leaves. Consequently, all examined mRNAs remarkably increased in senescent leaves, where the maximal magnitude of elevation for artemisinin biosynthetic transcripts, *CYP71AV1, ADS* and *DBR2* mRNAs, are 51.2, 25.5 and 14.8 folds compared with green leaves. In particular, *DBR2* and *ADS* mRNAs presented as abundant as 40×10^{-5} and 10×10^{-5} (**Fig. 3A** and **3B**) in senescent leaves, much higher than those in green leaves during the whole developmental stage. Moreover, also in senescent leaves, other three cytosolic pathway transcripts, *SS, HMGR* and *FDS* mRNAs, increased up to 11.2, 7.8 and 3.7 folds, while two plastidial pathway transcripts, *DXR* and *DXS* mRNAs, increased 18.5- and 11.1-fold. These results have unambiguously demonstrated that senescence leads to global activation of both cytosolic and plastidic pathway genes, in which the greatest extent of upregulation by senescence occurs in artemisinin biosynthetic genes investigated.

To further reveal the post-transcriptional and translational control fashions of artemisinin biosynthetic genes, ADS, CYP71AV1 and CPR enzymes in pre- and post-blooming *A. annua* plants were quantified by enzyme-linked immunosorbent assay. Prior to blooming, the maximal concentration of three enzymes are low (**Fig. 4A**). After blooming, these enzymes started to moderately increase in an organ-specific manner (**Fig. 4B**). With a same trend as corresponding mRNAs, three enzymes synchronously increased in senescent leaves, where they had approximately two-fold increments although ADS and CYP71AV1 were more copious than CPR. Not surprisingly, there may be a synergistic impact of senescence on upregulation of artemisinin biosynthetic genes at

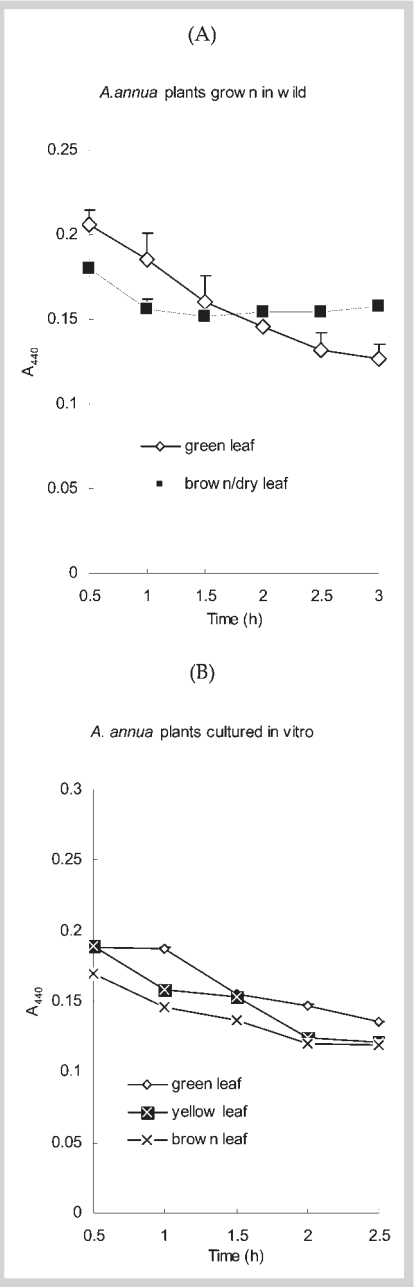

Fig. 5 The time course of $^1O_2$ emission from leaves of *A. annua* plants grown in the wild in September, 2008 (**A**) and from leaves of *A. annua* plants cultured *in vitro* (**B**).

transcriptional and translational levels, even though a higher level of the specific mRNA does not essentially lead to an equally higher concentration of the corresponding enzyme.

Within this context, senescent leaves were expected to accumulate more artemisinin than green leaves. Indeed, senescent leaves produced 8.07 ± 0.47 mg of artemisinin/g dry weight, while green leaves gave rise to only 5.43 ± 0.21 mg of artemisinin/g dry weight ($Y = 0.4833X + 0.0079$, $R^2 = 0.9988$). Therefore, elevated levels of *ADS, CYP71AV1* and *CPR* mRNAs as well as ADS, CYP71AV1 and CPR enzymes closely correlated with enhanced artemisinin production in senescent leaves, strongly suggesting that unidentified inducers might exert a critical role on activating artemisinin biosynthetic genes during senescence.

Considering that the oxidative stress response may emerge throughout ongoing senescence, both senescent and green leaves were collected from *A. annua* plants for monitoring their time-course changes of $^1O_2$ burst during which a lower absorbance at 440 nm indicates a higher level of $^1O_2$. Of wild-grown plants, brown and dry leaves emit more $^1O_2$ than green leaves within a duration of 2 h-detection, whereas after a 2 h-session of detection green leaves even released more $^1O_2$ than senescent leaves. Such a dual-phase mode of $^1O_2$ emission may be attributed to the presence of endogenous $^1O_2$-quenchers, for instance, carotenoids in plastids. Namely, extensive light should lead to senescent leaves with a diminishing capacity of photosynthetic electron transport emitting more $^1O_2$ than green leaves in the first phase (from 0–2 h), whereas green leaves with a continuous photosynthetic activity would release a stable baseline level of $^1O_2$ in the second phase (from 2–3 h) (**Fig. 5A**). On cultured plants, yellow and brown leaves released more $^1O_2$ than green leaves during the 2.5 h-duration of assay and also demonstrated a dual-phase effect after the 2.5 h-duration of assay (**Fig. 5B**).

It was further expected that oxidative stress conditions that evoke $^1O_2$ emission should simulate senescence to induce overexpression of terpene biosynthetic genes. Based on this assumption, as many as nine types of physical and chemical stress treatments that mimic adverse environments were applied to clarify the oxidative stress-induced expression patterns of seven cytosolic MVA pathway genes and two non-MVA pathway genes that would be directly or indirectly engaged in artemisinin biosynthesis.

In the physical stress group, waterlogging – causing hypoxia showed a strong inductivity to *DBR2* gene, in which treatment by hydration (waterlogging) or rehydration following dehydration (drought) allowed *DBR2* mRNA to rise for 13.8 folds or 38.2 folds over the control level, while low temperature or UV light conferred *DBR2* mRNA elevation of only two- or fourfold (**Fig. 6A**). In regard to the chemical stress group, yeast extracts induced a higher level of *DBR2* mRNA, accounting to 20.7 folds higher as the control (**Fig. 6B**). Upon exposure to low temperature or UV light, *ADS* mRNA increased up to 35.6 folds or 14.2 folds compared with the control. While hypoxia (e.g., waterlogging and rehydration) seemed not to impact *ADS* gene, dehydration endorsed elevation of *ADS* mRNA for 15.5 folds compared with the control. Following exposure to low temperature, UV light, waterlogging and rehydration, *CPR* mRNA increased for only about two to three folds over the control level.

The chilling-induced *DXS* mRNA level was elevated for twofold (**Fig. 7A**). *CYP71AV1* mRNA showed 3.7-, 5.0- or 6.9-fold increases over the control after induction by low temperature, UV light or waterlogging. Chilling- or UV-induced *HMGR* mRNAs demonstrated four- or twofold increases higher than the control. While *DXR* gene was solely inducible by low temperature, *FDS* gene was inducible by low temperature, heat shock and UV. Nonetheless, only a relative low mRNA level accumulated for each of these genes when compared with other genes (**Fig. 7B**). By the present treatments, however, *SS* gene was not at all significantly inducible (**Fig. 7C**).

As a brief conclusion, overexpression of artemisinin biosynthetic genes occurs in senescent leaves typically simulated by several oxidative stress circumstances that emit $^1O_2$. For example, temperature stress and water stress can induce artemisinin biosynthetic genes and enhance artemisinin production as well.

Discussion

The striking feature of terpenes as scavengers of reactive oxygen species has been demonstrated by Velikova et al. [26], who observed that a physiological level of endogenous terpenes in

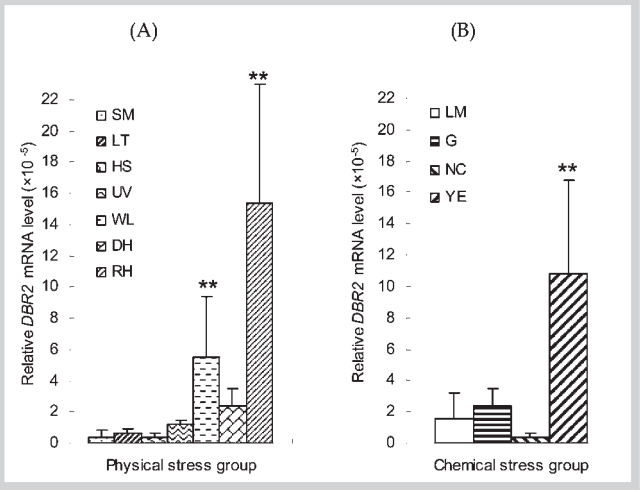

Fig. 6 Quantification of *DBR2* mRNAs in cultural 30-day-old *A. annua* plants as exposed to physical and chemical stresses. SM: solid medium; LT: low temperature; HS: heat shock; UV: ultraviolet light; WL: waterlogging; DH: dehydration; RH: rehydration; LM: liquid medium; G: glucose; NC: NaCl; YE: yeast extracts. **A** The physical stress group; **B** The chemical stress group. Copy numbers of each mRNA were estimated according to the regression formula from the standard curve of an individual gene. For 18S rDNA, $Y = -3.080155X + 37.565701$, $R^2 = 0.997668$ (physical stresses) and $Y = -2.974454X + 34.638035$, $R^2 = 0.991175$ (chemical stresses); For *DBR2*, $Y = -3.678958X + 40.286537$, $R^2 = 0.999076$ (physical stresses) and $Y = -3.748647X + 42.083920$, $R^2 = 0.998887$ (chemical stresses). Double asterisks (**) represent a very significant statistical difference ($p < 0.01$).

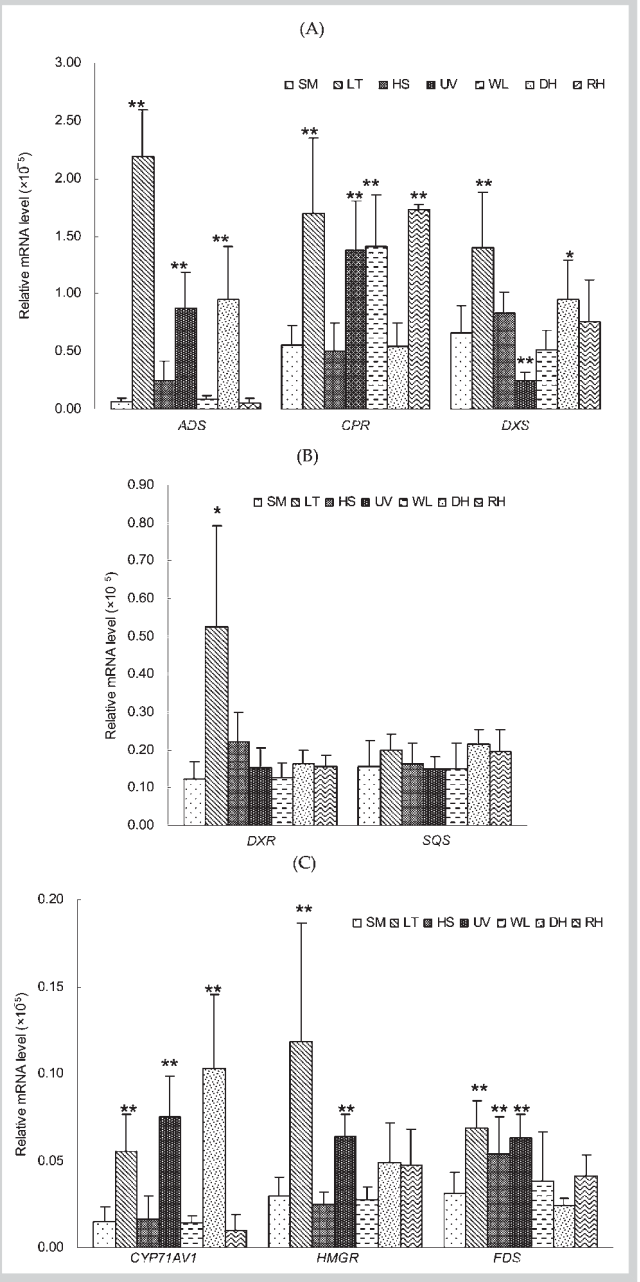

Fig. 7 Quantification of artemisinin biosynthesis responsible mRNAs in cultural 30-day-old *A. annua* plants as exposed to physical stresses. SM: solid medium; LT: low temperature; HS: heat shock; UV: ultraviolet light; WL: waterlogging; DH: dehydration; RH: rehydration. **A** The high inducible mRNAs; **B** the moderately inducible or non-inducible mRNAs; **C** the low inducible mRNAs. Copy numbers of each mRNA were estimated according to the regression formula from the standard curve of an individual gene. For 18S rDNA, $Y = -3.080155X + 37.565701$, $R^2 = 0.997668$; For *HMGR*, $Y = -3.254588X + 40.334274$, $R^2 = 0.999570$; For *FPS*, $Y = -3.370094X + 36.101112$, $R^2 = 0.996038$; For *ADS*, $Y = -3.156213X + 38.538124$, $R^2 = 0.997035$; For *CYP71AV1*, $Y = -3.446953X + 37.827961$, $R^2 = 0.999090$; For *CPR*, $Y = -3.298541X + 32.455555$, $R^2 = 0.998452$; For *SQS*, $Y = -3.296258X + 41.160362$, $R^2 = 0.997671$; For *DXS*, $Y = -3.213989X + 36.574371$, $R^2 = 0.999039$; For *DXR*, $Y = -3.06169X + 36.108486$, $R^2 = 0.999781$. The single asterisk (*) represents a significant statistical difference ($p < 0.05$); Double asterisks (**) represent a very significant statistical difference ($p < 0.01$).

Phragmites australis offers protection against $^1O_2$. In *A. annua*, it has been suggested that DHAA may function as a $^1O_2$ scavenger that reacts with $^1O_2$ to give rise to an unstable DHAA hydroperoxide, which is eventually autooxidized to artemisinin [13, 14]. Due to the ubiquitous presence of $^1O_2$, *A. annua* is assumed to continuously synthesize DHAA throughout its vegetative and reproductive growth stages. Although the maximal content of artemisinin is exclusively achieved after leaves turn brown, DHAA accumulates in a high quantity early in the leaf cycle [16]. By final harvests, a larger proportion of artemisinin in senescent leaves than that in green leaves was detected by Lommen et al. [15].

The present study has apparently shown that artemisinin biosynthetic genes are highly activated in senescent leaves (**Fig. 1**), and *DBR2* mRNA is always one of the most abundant transcripts in both green and senescent leaves although *DBR2* gene is extremely upregulated in senescent leaves. One can image that DHAA that has accumulated in green leaves could not completely convert to artemisinin due to a low $^1O_2$ level during the early vegetative growth stage. Given the knowledge that DHAA is actually a high-level intermediate in expanding leaves [15], it would be reasonable to predict that the excessive DHAA might, in a feedback manner, inhibit activities of upstream key enzymes on the MVA pathway. As such, mRNAs responsible for terpene biosynthesis are of course rare transcript species in green leaves and possess less variations among distinct organs (**Fig. 2**). As an irreversible reaction, for example, the HMGR-catalyzed reaction has been confirmed to be a rate-limiting step and an important checkpoint on the MVA pathway [27]. Although such a role for DHAA is still speculative at this time, suppression of *ADS* gene in young leaves of *A. annua* has been noted by Bouwmeester et al. [7] and subsequently confirmed by our group [23]. In contrast, senescent leaves demonstrate strong inductivities to both MVA

and non-MVA pathway genes, by not only elevating levels of *HMGR, FDS, ADS, CYP71AV1, CPR, DBR2, DXS* and *DXR* mRNAs (**Fig. 3**), but also by increasing concentrations of ADS, CYP71AV1 and CPR enzymes and simultaneously enhancing artemisinin production (**Fig. 4**).

By analyzing transcriptional profiles of senescent *Triticum aestivum* leaves, Gregersen and Holm [28] found that more than 140 genes that encompass those encoding antioxidant enzymes such as aconitase and citrogenase are upregulated to protect cells from oxidative damage. This result has indicated that reactive oxygen species-induced genes responsible for antioxidation must be overexpressed upon subjecting plants to oxidative stress. In our investigation, a comparison of the strength for $^1O_2$ burst among leaves of *A. annua* has proved that senescent leaves release more $^1O_2$ than green leaves (**Fig. 5**), hence confirming that senescence is capable of invoking $^1O_2$ burst. Therefore, it is reasonable that abiotic and biotic stresses that trigger $^1O_2$ burst should induce overexpression of artemisinin biosynthetic genes.

Apart from other effectors under study, *DBR2* gene is highly inducible by yeast extracts, which were used as analogues to fungal elicitors mimicking pathogen infection [29]. Interestingly, *ADS* gene is also upregulated by yeast extracts in our investigation (data not shown). Artemisinin production in *A. annua* hairy roots is enhanced by the elicitor extracted from the endophytic *Colletotrichum* sp. [30]. Besides, exposure of *Panax ginseng* to fungal elicitors invokes transient $^1O_2$ release [31]. These results are helpful to uncover a plausible relationship between accelerated $^1O_2$ burst and promoted artemisinin biosynthesis as a consequence of action by yeast extracts. Moreover, the correlation of chilling exposure with $^1O_2$ burst has been addressed in *Cucumis sativus* L. [32]. In our recent work, chilling exposure was found to trigger $^1O_2$ emission in transgenic *A. annua* plants that express an antisense *SS* gene [33]. As described in the present work, chilling stress indeed upregulates all studied cytosolic and plastidial pathway genes (**Figs. 6** and **7**).

Although several oxidative stress conditions can simulate senescence to activate overexpression of some relevant genes, the magnitude of oxidative stress-induced mRNAs is lower than that of senescence-induced mRNAs. For example, senescence leads to *DBR2* mRNA elevation up to 40×10^{-5}, whereas yeast extracts or rehydration only allow *DBR2* mRNA elevation to 10×10^{-5} or 15×10^{-5}. This implies that activation of *DBR2* gene may require a higher level of $^1O_2$ and senescence can evoke much more $^1O_2$ than oxidative stress. The $^1O_2$-quenching ability of naturally occurring carotenoids in plastids has been validated [18], so senescence perhaps potently affects carotenoid biosynthesis. It seems likely that less carotenoids should be synthesized and more $^1O_2$ be emitted when the plastidial non-MVA pathway towards carotenoid biosynthesis is attenuated after senescence or blocked by a metabolic inhibitor. In this regard, our preliminary analysis has indicated that incubation of *A. annua* with plastid-specific non-MVA pathway inhibitors, fosmidomycin and fluridon, exceedingly accelerates the transcription of *DBR2* gene by 80- and 15-fold elevations, respectively (to be issued elsewhere).

The signalling of $^1O_2$ and $^1O_2$-induced activation of nuclear genes are still not fully understood. Because $^1O_2$ is very unstable and unlikely to move far away, a question about how the $^1O_2$ signal being generated within plastids is transmitted across membranes would be raised. In this regard, Laloi et al. [34] and Lee et al. [35] have indicated that the $^1O_2$ signal originating in plastids can be transduced into nuclei via two protein factors, EXECUTER-1 and EXECUTER-2, and initiates the transcription of $^1O_2$-responsive genes. The primary function of $^1O_2$ is believed to induce a stress-related signaling cascade that encompasses numerous signaling pathways known to be activated by pathogen attack, wounding, light and drought stresses [36].

We herein confirm that *A. annua* has evolved a fine-tuned antioxidant mechanism, by which carotenoids, DHAA and other $^1O_2$-scavengers are combined to promptly quench the excessive $^1O_2$ that emits during senescence or under oxidative stress. An overall tendency of artemisinin accumulation in *A. annua* is organ-specific, season-dependent, but more accurately, $^1O_2$-inducible. These rather astonishing findings along with other useful knowledge [37] should pave an avenue towards thorough elucidation of artemisinin overproduction and facilitate its practical utilization in the medicinal agriculture of *A. annua* cultivation.

Acknowledgements

We thank Zeng LX, Guo XX and Zhang PZ for their helpful assistance in the experiment. This work was supported by the grants from the Natural Science Foundation of China (NSFC) (30672614 and 30870072) and from the Scientific Development Project of Guangdong, China (2007B031404008).

References

1 *Klayman DL.* Qinghaosu (artemisinin): an antimalarial drug from China. Science 1985; 228: 1049–1055
2 *Bertea CM, Freije JR, van der Woude H, Verstappen FWA, Perk L, Marquez V, de Kraker JW, Posthumus MA, Jansen BJM, de Groot A, Franssen MCR, Bouwmeester HJ.* Identification of intermediates and enzymes involved in the early steps of artemisinin biosynthesis in *Artemisia annua.* Planta Med 2005; 71: 40–47
3 *Covello PS, Teoh KH, Polichuk DR, Reed DW, Nowak G.* Functional genomics and the biosynthesis of artemisinin. Phytochemistry 2007; 68: 1864–1871
4 *Zeng QP, Qiu F, Yuan L.* Production of artemisinin by genetically modified microbes. Biotechnol Lett 2008; 30: 581–592
5 *Zeng QP, Yang RY, Feng LL, Yang XQ.* Genetic and environmental regulation and artificial metabolic manipulation for artemisinin biosynthesis. In: Richter FW, editor. Biotechnology: research, technology and applications. New York: Nova Science Publishers, Inc.; 2008: 159–210
6 *Towler MJ, Weathers PJ.* Evidence of artemisinin production from IPP stemming from both the mevalonate and the non-mevalonate pathways. Plant Cell Rep 2007; 26: 2129–2136
7 *Bouwmeester HJ, Wallaart TE, Janssen MHA, van Loo B, Jansen BJM, Posthumus MA, Schmidt CO, de Kraker JW, Konig WA, Fransen MC.* Amorpha-4,11-diene synthase catalyses the first probable step in artemisinin biosynthesis. Phytochemistry 1999; 52: 843–854
8 *Teoh KH, Polichuk DR, Reed DW, Nowak G, Covello PS. Artemisia annua* L. (Asteraceae) trichome-specific cDNAs reveal CYP71AV1, a cytochrome P450 with a key role in the biosynthesis of the antimalarial sesquiterpene lactone artemisinin. FEBS Lett 2006; 580: 1411–1416
9 *Ro DK, Paradise EM, Ouellet M, Fisher KJ, Newman KL, Ndungu JM, Ho KA, Eachus RA, Ham TS, Kirby J, Chang MCY, Withers ST, Shiba Y, Sarpong R, Keasling JD.* Production of the antimalarial drug precursor artemisinic acid in engineered yeast. Nature 2006; 440: 940–943
10 *Lindahl AL, Olsson ME, Mercke P, Tollbom Ö, Schelin J, Brodelius M, Brodelius PE.* Production of the artemisinin precursor amorpha-4,11-diene by engineered *Sacharomyces cerevisiae*. Biotechnol Lett 2006; 28: 571–580
11 *Chang MCY, Eachus RA, Trieu W, Ro DK, Keasling JD.* Engineering *Escherichia coli* for production of functionalized terpenoids using plant P450s. Nat Chem Biol 2007; 3: 274–277
12 *Zhang YS, Teoh KH, Reed DW, Maes L, Goossens A, Olson DJH, Ross ARS, Covello PS.* The molecular cloning of artemisinic aldehyde Δ11 (13) reductase and its role in glandular trichome-dependent biosynthesis of artemisinin in *Artemisia annua*. J Biol Chem 2008; 283: 21 501–21 508
13 *Sy LK, Brown GD.* The mechanism of the spontaneous autoxidation of dihydro-artemisinic acid. Tetrahedron 2002; 58: 897–908

14 *Wallaart TE, van Uden W, Lubberink HGM, Woerdenbag HJ, Pras N, Quax WJ.* Isolation and identification of dihydroartemisinic acid from *Artemisia annua* and its possible role in the biosynthesis of artemisinin. J Nat Prod 1999; 62: 430–433

15 *Lommen WJM, Schenk E, Bouwmeester HJ, Verstappen FWA.* Trichome dynamics and artemisinin accumulation during development and senescence of *Artemisia annua* leaves. Planta Med 2006; 72: 336–345

16 *Sangwan RS, Agarwal K, Luthra R, Thakur RS, Sangwan NS.* Biotransformation of arteannuic acid into arteannuin B and artemisinin in *Artemisia annua*. Phytochemistry 1993; 34: 1301–1302

17 *Nair MSR, Basile DV.* Bioconversion of arteannuin B to artemisinin. J Nat Prod 1993; 56: 1559–1566

18 *Hirayama O, Nakamura K, Hamada S, Kobayashi Y.* Singlet oxygen quenching ability of naturally occurring carotenoids. Lipids 1994; 29: 149–150

19 *Wallaart TE, Bouwmeester HJ, Hille J.* Amorpha-4,11-diene synthase: cloning and functional expression of a key enzyme in the biosynthetic pathway of the novel antimalarial drug artemisinin. Planta 2001; 212: 460–465

20 *Yin LL, Zhao C, Huang Y, Yang RY.* Abiotic stress-induced expression of artemisinin biosynthesis genes in *Artemisia annua* L. Chin Appl Environ Biol 2008; 14: 1–5

21 *Zeng QP, Zhao C, Yin LL, Yang RY, Zeng XM, Huang Y, Feng LL, Yang XQ.* Cloning of artemisinin biosynthetic cDNAs and novel ESTs and quantification of low temperature-induced gene overexpression. Sci China Ser C (Life Sci) 2008; 51: 232–244

22 *Lommen WJM, Elzinga S, Verstappen FWA, Bouwmeester HJ.* Artemisinin and sesquiterpene precursors in dead and the green leaves of *Artemisia annua* L. crops. Planta Med 2007; 73: 1133–1139

23 *Yang RY, Feng LL, Yang XQ, Yin LL, Xu XL, Zeng QP.* Quantitative transcript profiling reveals down-regulation of a sterol pathway relevant gene and overexpression of artemisinin biogenetic genes in transgenic *Artemisia annua* plants. Planta Med 2008; 74: 1510–1516

24 *Zeng QP, Zeng XM, Yin LL, Yang RY, Feng LL, Yang XQ.* Quantification of three key enzymes involved in artemisinin biogenesis in *Artemisia annua* by polyclonal antisera-based ELISA. Plant Mol Biol Rep 2009; 27: 50–57

25 *Pedraza-Chaverrí J, Barrera D, Maldonado PD, Chirino YI, Macías-Ruvalcaba NA, Medina-Campos ON, Castro L, Salcedo MI, Hernandez-Pando R.* S-allylmercaptocysteine scavenges hydroxyl radical and singlet oxygen *in vitro* and attenuates gentamicin- induced oxidative and nitrosative stress and renal damage *in vivo*. EMC Clin Pharmacol 2004; 4: 5

26 *Velikova V, Edreva A, Loreto F.* Endogenous isoprene protects *Phragmites australis* leaves against singlet oxygen. Physiol Plant 2004; 122: 219–225

27 *Chappell J, Wolf F, Proulx J, Cuellar R, Saunders C.* Is the reaction catalyzed by 3-hydroxyl-3-methylglutaryl coenzyme A reductase a rate-limiting step for isoprenoid biosynthesis in plant? Plant Physiol 1995; 109: 1337–1343

28 *Gregersen PL, Holm PB.* Transcriptome analysis of senescence in the flag leaf of wheat (*Triticum aestivum* L.). Plant Biotechnol J 2007; 5: 192–206

29 *Menke FLH, Parchmann S, Mueller MJ, Kijne JW, Memelink J.* Involvement of the octadecanoid pathway and protein phosphorylation in fungal elicitor-induced expression of terpenoid indole alkaloid biosynthetic genes in *Catharanthus roseus*. Plant Physiol 1999; 119: 1289–1296

30 *Wang JW, Zhang Z, Tan RX.* Stimulation of artemisinin production in *Artemisia annua* hairy roots by the elicitor from the endophytic *Colletotrichum* sp. Biotechnol Lett 2001; 23: 857–860

31 *Xu X, Hu X, Neill SJ, Fang J, Cai W.* Fungal elicitor induces singlet oxygen generation, ethylene release and saponin synthesis in cultured cells of *Panax ginseng* C. A. Meyer. Plant Cell Physiol 2005; 46: 947–954

32 *Wise RR, Naylor AW.* Chilling-enhanced photooxidation: evidence for the role of singlet oxygen and superoxide in the breakdown of pigments and endogenous antioxidants. Plant Physiol 1987; 83: 278–282

33 *Feng LL, Yang RY, Yang XQ, Zeng XM, Lu WJ, Zeng QP.* Synergistic re-channeling of mevalonate pathway for artemisinin overproduction in transgenic *Artemisia annua*. Plant Sci 2009; 177: 57–67

34 *Laloi C, Stachowiak M, Pers-Kamczyc E, Warzych IM, Apel K.* Cross-talk between singlet oxygen- and hydrogen peroxide-dependent signalling of stress responses in *Arabidopsis thaliana*. Proc Natl Acad Sci USA 2007; 104: 672–677

35 *Lee KP, Kim C, Landgraf F, Apel K.* EXECUTER1- and EXECUTER2-dependent transfer of stress-related signals from the plastid to the nucleus of *Arabidopsis thaliana*. Proc Natl Acad Sci USA 2007; 104: 10270–10275

36 *Laloi C, Przybyla D, Apel K.* A genetic approach towards elucidating the biological activity of different reactive oxygen species in *Arabidopsis thaliana*. J Exp Bot 2006; 57: 1719–1724

37 *Wallaart TE, Pras N, Beekman AC, Quax WJ.* Seasonal variation of artemisinin and its biosynthetic precursors in plants of *Artemisia annua* of different geographical origin: proof for the existence of chemotypes. Planta Med 2000; 66: 57–62